

# ENERGY SHAPING AND INTERCONNECTION AND DAMPING ASSIGNMENT CONTROL IN THE BOND GRAPH DOMAIN

Alejandro Donaire and Sergio Junco  
Departamento de Electrónica - Universidad Nacional de Rosario  
CONICET, Argentine National Council of Scientific and Technical Research  
Riobamba 245 bis, S2000EKE Rosario, Argentina  
E-mail: {adonaire, sjunco}@fceia.unr.edu.ar

## KEYWORDS

Bond Graphs, Port-Controlled Hamiltonian Systems, Nonlinear Control, Energy Shaping, Interconnection and Damping Assignment.

## ABSTRACT

This paper presents an interpretation in the Bond Graph domain of the Energy Shaping and Interconnection and Damping Assignment control methods, developed for the well-known Port-Controlled Hamiltonian Systems with Dissipation. In order to have a stable equilibrium at a prespecified state, the energy function is modified by adding storage elements to the BG such that the closed-loop system element has a minimum at that state. A new dissipation function is assigned changing the  $R$ -field and its interconnection with the rest of the Bond Graph. A desired power conserving interconnection structure is reached through the suitable insertion of power bonds among junctions. Energy shaping, interconnection and damping assignment are performed in a so called Target Bond Graph. The control law is determined by a set of partial differential equations derived from the plant and the Target Bond Graph.

## INTRODUCTION

Energy Shaping (ES) and Interconnection and Damping Assignment (IDA) are known control theoretical methods developed especially (but not exclusively) for physical systems represented as Port-Controlled Hamiltonian System with Dissipation (PCHD) (van der Schaft 2000; Ortega et al. 2002). This class of models has shown to be suitable for control system synthesis based in passivity theory, like ES and IDA methods, because they express explicitly the energy storage and dissipation phenomena, as well as the power conserving exchange between the components of the system.

The Bond Graph (BG) formalism is very successful for system modeling and simulation (Karnopp et al. 2000). The graphical description of BGs exhibits the power conserving interconnection structure between the energy storages, the contribution of each storage to the energy function via its potential or kinetic energy, the energy dissipation structure, and the power exchange with the environment. Moreover, the assignment of causality to a BG provides mathematical tools for system level analysis (Dauphin-Tanguy et al. 1999; Bertrand et al. 2001).

These properties of BG models motivated this research, which focuses in the translation into the BG language of control methods originally formulated in a generic mathematical setup for PCHD systems. Previous results used in this paper are the derivation of PCHD models from BGs (Donaire and Junco 2005) and the idea of Target Bond Graphs (Junco 2004). Yielding closely related results, an independent approach to the same problem has been reported in (Vink 2005).

The remaining of the paper is organized as follows: first, an account of ES and IDA on PCHD is given, and the equivalences between both formalisms is given. Next, the main result is addressed, i.e., performing ES and IDA control methods on the BG domain. Two realistic examples illustrating the methodology are exposed subsequently. Next, the theoretical results are confirmed by simulation. Finally, some conclusions are drawn and the future research is discussed.

## BACKGROUND

### PCHD Systems

A system whose dynamics can be represented in form (1) is called a PCHD (van der Schaft 2000).

$$\begin{aligned}\dot{x} &= [J(x) - R(x)] \frac{\partial H}{\partial x}(x) + g(x)u \\ y &= g^T(x) \frac{\partial H}{\partial x}(x)\end{aligned}\quad (1)$$

The state variables  $x \in \mathfrak{R}^n$  are the energy variables ( $n$  is the system order), the smooth function  $H(x): \mathfrak{R}^n \rightarrow \mathfrak{R}$  represents the total energy stored in the system, and  $u, y \in \mathfrak{R}^m$  are the input- and output-port power variables, respectively. Inputs and outputs are conjugate variables so that their product represents the power exchanged between the system and the environment. The input vector  $u$  is modulated by the  $n \times m$  matrix  $g(x)$  which also defines the output vector  $y$ . The  $n \times n$  skew-symmetric matrix  $J(x) = -J^T(x)$  reveals the power-conserving interconnection structure in the model, while the dissipation structure is captured by the symmetric matrix  $R = R^T \geq 0$ . Both matrices depend smoothly on  $x$ .

There are systems where the control acts through the interconnection structure (e.g., power electronic devices when the switched system behavior can be approximated by a smooth system). For this kind of

systems, the model (1) can be further generalized by (2) (Ortega et al 2002), where  $J(x,u) = -J^T(x,u)$ .

$$\dot{x} = [J(x,u) - R(x)] \frac{\partial H}{\partial x}(x) + g(x,u) \quad (2)$$

A most important property of PCHD systems is its I-O passivity, with the energy  $H$  of the system being the storage function and  $s=y^T u$  the supply rate (van der Schaft 2000). The power continuity equation (3), due to the properties of the matrix  $J$ , shows that the excess of supplied over stored energy is dissipated by the action of  $R(x)$  because of its symmetry and positive definiteness.

$$\begin{aligned} \dot{H}(x) &= \left[ \frac{\partial H}{\partial x} \right]^T \dot{x} = \left[ \frac{\partial H}{\partial x} \right]^T [J(x) - R(x)] \frac{\partial H}{\partial x} + \left[ \frac{\partial H}{\partial x} \right]^T g(x)u \\ &= - \left[ \frac{\partial H}{\partial x} \right]^T R(x) \frac{\partial H}{\partial x} + y^T u \end{aligned} \quad (3)$$

Integrating (3) over an arbitrary time-interval  $[t_0, t_1]$  results in the well-known *dissipative inequality* below, which ascertains the passive properties of PCHD systems (Willems 1972).

$$H(x(t_1)) \leq H(x(t_0)) + \int_{t_0}^{t_1} y^T u dt$$

### Control of PCHD Systems

Control design techniques such as *Energy Shaping* (ES) and *Interconnection and Damping Assignment* (IDA) have been developed with the help of the explicit information of the energy function, and the properties of interconnection and dissipation of PCHD systems.

The idea of ES consists in shaping the energy function of the plant in order to obtain a new closed loop energy function that has a minimum point at the desired state, preserving the interconnection structure and the dissipative function of the plant. Then, the closed-loop system will preserve the PCHD form with a stable equilibrium point in the energy minimum. Proposition 1 presents formally the ES method.

*Proposition 1* (van der Schaft 2000). Consider that for the PCHD (1) it is possible to find a feedback control law  $u = \alpha(x)$  and a vector function  $K(x)$  satisfying

$$[J(x) - R(x)]K(x) = g(x)\alpha(x)$$

such that,

$$\begin{aligned} i) \quad & \frac{\partial K_i}{\partial x_j}(x) = \frac{\partial K_j}{\partial x_i}(x), \quad i, j=1, \dots, n \\ ii) \quad & K(x^*) = -\frac{\partial H}{\partial x}(x^*) \\ iii) \quad & \frac{\partial K}{\partial x}(x^*) > -\frac{\partial H}{\partial x}(x^*) \end{aligned} \quad (4)$$

with the  $i$ -th column of the  $n \times n$  matrix  $\partial K / \partial x$  given by  $\partial K_i / \partial x$ ; and  $\partial^2 H / \partial x^2(x^*)$  denoting the Hessian matrix of  $H$  at  $x^*$ .

Then the closed-loop system (5) is a PCHD having  $x^*$  as a stable equilibrium.

$$\dot{x} = [J(x) - R(x)] \frac{\partial H_d}{\partial x}(x) \quad (5)$$

Here,  $H_d = H + H_a$  is the desired Hamiltonian, and  $H_a$  is such that  $K(x) = \partial H_a / \partial x(x)$ .  $\square$

If it were necessary to shape not only the energy function but also to assign a new dissipative function and/or a new interconnection structure, ES results insufficient. Then, the IDA method (Proposition 2) has to be applied.

*Proposition 2* (Ortega et al., 2002). Let the PCHD (2) be characterized by  $J(x,u)$ ,  $R(x)$ ,  $H(x)$ ,  $g(x,u)$ , and a desired equilibrium  $x^* \in \mathfrak{R}^n$  to be stabilized. Assume it can be found functions  $\beta(x)$ ,  $J_a(x)$ ,  $R_a(x)$  and a vector function  $K(x)$  satisfying

$$\begin{aligned} & [J(x, \beta(x)) + J_a(x) - (R(x) + R_a(x))]K(x) \\ & = -[J_a(x) - R_a(x)] \frac{\partial H}{\partial x}(x) + g(x, \beta(x)) \end{aligned} \quad (6)$$

and such that

i) (*Structure Preservation*) The closed-loop is a PCHD

$$\begin{aligned} J_d(x) &:= J(x, \beta(x)) + J_a(x) = -[J(x, \beta(x)) + J_a(x)]^T, \\ R_d(x) &:= R(x) + R_a(x) = [R(x) + R_a(x)]^T \geq 0 \end{aligned} \quad (7)$$

ii) (*Integrability*)  $K(x)$  is the gradient of a scalar function. That is,

$$\frac{\partial K}{\partial x}(x) = \left[ \frac{\partial K}{\partial x}(x) \right]^T \quad (8)$$

iii) (*Equilibrium Assignment*)  $K(x)$ , at  $x^*$ , verifies

$$K(x^*) = -\frac{\partial H}{\partial x}(x^*) \quad (9)$$

iv) (*Lyapunov Stability*) The Jacobian of  $K(x)$ , at  $x^*$ , satisfies the bound

$$\frac{\partial K}{\partial x}(x^*) > -\frac{\partial^2 H}{\partial x^2}(x^*) \quad (10)$$

Under these conditions, the closed-loop system defined by  $u = \beta(x)$  will be the PCHD (11)

$$\dot{x} = [J_d(x) - R_d(x)] \frac{\partial H_d}{\partial x}(x) \quad (11),$$

where  $H_d(x) = H(x) + H_a(x)$  and  $\partial H_a / \partial x(x) = K(x)$ . Furthermore,  $x^*$  will be a (locally) stable equilibrium of the closed-loop. In addition, it will be asymptotically stable if the largest invariant set under the closed-loop dynamics contained in  $\{x \in \mathfrak{R}^n \mid [(\partial H_d / \partial x)(x)]^T R_d(x) (\partial H_d / \partial x)(x) = 0\} = \{x^*\}$ .  $\square$

## Obtaining PCHD Models from BG

The Junction Structure (JS) equations (12), that provide the BG interconnection structure, constitute, along with the component constitutive laws (Table 1), the BG-Standard Implicit Form (BG-SIF). Using the BG energy properties and the BG-SIF, it is possible to find an equivalence between BG and PCHD variables, as well as some properties that link both representations (Donaire and Junco 2005).

$$\begin{bmatrix} \dot{X}_i \\ Z_d \\ D_i \end{bmatrix} = \begin{bmatrix} S_{11} & S_{12} & S_{13} & S_{14} \\ S_{21} & S_{22} & S_{23} & S_{24} \\ S_{31} & S_{32} & S_{33} & S_{34} \end{bmatrix} \begin{bmatrix} Z_i \\ \dot{X}_d \\ D_o \\ U \end{bmatrix} \quad (12)$$

Table 1. Constitutive Laws

NON LINEAR	LINEAR
$Z_i = f(X_i)$	$Z_i = FX_i$
$D_o = l(X_i)D_i$ <i>multiplicative modulated Resistors</i>	$D_o = LD_i$
$X_d = g(Z_d)$	$X_d = GZ_d$

The equivalence of PCHD and BG variables is shown in Table 2, assuming BGs with all the storages in integral causality assignment (ICA). For the case of storages in derivative causality see (Donaire and Junco 2005).

Table 2. Equivalence of variables

PCHD MODEL		BG MODEL	
State vector	$x$	$\Leftrightarrow$	$X_i$ Vector of energy variables $\equiv$ state vector
Energy gradient respect to the state vector	$\frac{\partial H}{\partial x}$	$\Leftrightarrow$	$Z_i$ Output vector of the storage field in ICA
Derivative of the state vector	$\dot{x}$	$\Leftrightarrow$	$\dot{X}_i$ Input vector of the storage field in ICA

The PCHD (2) can be expressed in the BG domain as (13), with the PCHD structure matrices given by (14)

$$\begin{aligned} \dot{X}_i = & \left\{ S_{11} + S_{13}l(X_i)[I - S_{33}l(X_i)]^{-1} S_{31} \right\} Z_i + \\ & + \left\{ S_{14} + S_{13}l(X_i)[I - S_{33}l(X_i)]^{-1} S_{34} \right\} U \end{aligned} \quad (13)$$

$$\begin{aligned} J(x) - R(x) = & S_{11} + S_{13}l(X_i)[I - S_{33}l(X_i)]^{-1} S_{31} \\ g(x) = & S_{14} + S_{13}l(X_i)[I - S_{33}l(X_i)]^{-1} S_{34} \end{aligned} \quad (14)$$

In models without coupled resistors,  $J$  is solely determined by  $S_{11}$ , and  $R$  by  $S_{13}$ ,  $l(X_i)$  and  $S_{31}$ .

## ES AND IDA METHODS IN THE BG DOMAIN

This section interprets the ES and IDA methods in the BG domain. The technique of BG-prototyping (Junco

2004) yields a so-called Target BG (TBG), which here - somewhat differently as in the above reference- is defined as the inputless BG of the plant, to which elements have been suitably added in order to meet the closed-loop requirements, i.e., to shape the energy function and assign the interconnection structure and the dissipation function. As the TBG represents the desired closed-loop dynamics, the control law is to be determined as to emulate the effect of the added components, i.e., the action of the controlled modulated sources, MTFs and MGYs in the BG of the plant has to match the action of the elements added in the TBG.

## Energy Shaping on BG

Assuming all storages in ICA, the TBG is obtained as suggested in Fig. 1 via adding new storages -with constitutive laws to be determined- as follows: each new I-element shares its effort with each original I-element on an added common 0-junction-, and each new C-element shares its flow with each original C-element on an added common 1-junction. The co-energy variables of the storages (their outputs, see Table 2) are  $Z_i = \partial H / \partial X_i$  and  $Z_i^a = \partial H_a / \partial X_i^a = \partial H_a / \partial X_i$ , with  $H$  and  $H_a$  the stored energy in the original and the added elements, respectively, and their sum  $H_s$  the total desired energy. The JS and the  $R$ -Field do not change. Thus, the energy function is shaped and both the interconnection structure and the dissipative function are conserved. The inputs of the new and the original storages are the same,  $dX_i^a/dt = dX_i/dt$ , (subindex "i" stands for integral (causality), superindex "a" for added) and their energy variables are constrained to be identical, i.e.,  $X_i = X_i^a$ . Thus, the dynamics of the TBG is fully described by that of  $X_i$ , as given in (15) (cf. (13), and recall the inputless feature of the TBG and that the inputs from the storages to the JS are  $Z_i$  and  $Z_i^a$ ).

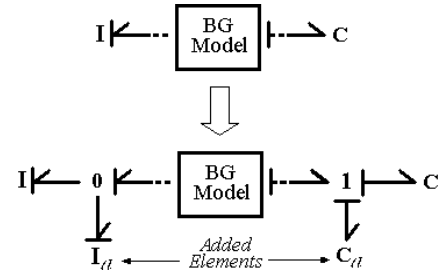


Figure 1. Adding Energy to BG model

$$\dot{X}_i = \left[ S_{11} + S_{13}l(X_i)(I - S_{33}l(X_i))^{-1} S_{31} \right] (Z_i + Z_i^a) \quad (15)$$

$$\text{with } Z_i = \frac{\partial H}{\partial X_i}(X_i), \quad Z_i^a = \frac{\partial H_a}{\partial X_i}(X_i), \quad Z_i^s = \frac{\partial H}{\partial X_i} + \frac{\partial H_a}{\partial X_i} = \frac{\partial H_s}{\partial X_i}$$

The control inputs must replicate the action of the added elements to achieve the dynamics of the TBG, which is expressed mathematically by the matching equation (16), obtained equating (13) and (15).

Summarizing this BG-ES technique: given a BG model (the plant), a TBG with the desired energy function satisfying (4) at the desired equilibrium point has to be

built. Then, the feedback control law determined by (16) forces a closed-loop PCHD system with the energy function (17), with a stable equilibrium at  $X_i^*$ , and the same interconnection structure and dissipative function as the original plant.

$$\left[ S_{14} + S_{13}l(X_i)(I - S_{33}l(X_i))^{-1}S_{34} \right] U = \left[ S_{11} + S_{13}l(X_i) \right. \quad (16)$$

$$\left. (I - S_{33}l(X_i))^{-1}S_{31} \right] \frac{\partial H_a}{\partial X_i} \quad (17)$$

$$H_s(X_i) = H(X_i) + H_a(X_i)$$

*Remark 1.* In general the constitutive law of the added elements are unknown, i.e. the added energy function is undetermined. Thus, (16) results in a set of Partial Differential Equations (PDEs) that gives a family of solutions for  $H_a$ . Then, the requirement of a minimum at the desired stable equilibrium determines the energy function to be added. The constitutive laws of each added elements can be calculated as the partial derivative of  $H_a$  with respect to the associated energy variable.

### Interconnection and Damping Assignment on BG

The IDA method is indicated when it is desirable to change the interconnection structure or the dissipative function (or both) as well as the energy function. This subsection shows how to assign the interconnection structure and the dissipative function in the BG, the energy function in BG-IDA being shaped as in BG-ES. The technique is based on the construction of a TBG as follows: the first step consist in adding storages to the original BG without inputs to shape the energy function. After that, the power conserving interconnection structure is modified by adding power bonds that change the gain of the causal paths between the storages, such that the desired interconnection structure is obtained. Finally, the desirable damping is attained by adding the necessary resistors and their interconnection with the rest of the BG.

This technique is illustrated on the Permanent Magnet Synchronous Motor of Fig. 2, as example. Adding the storages (dashed-line boxes) in the TBG of Fig. 3 modifies the energy function of the system. The interconnection structure is changed by adding the modulated gyrator connected by dashed bonds. With this new interconnection structure, the rotor speed is driven by the quadrature-axis modulated by the direct-axis flux. In this way the mechanical dynamics and the electrical dynamics in quadrature have no influence on the electrical direct-axis, thereby making simpler the direct flux control. Damping is assigned via the new resistor  $R^a$  and the added power bond that connect  $R^a$  with the rest of the BG.

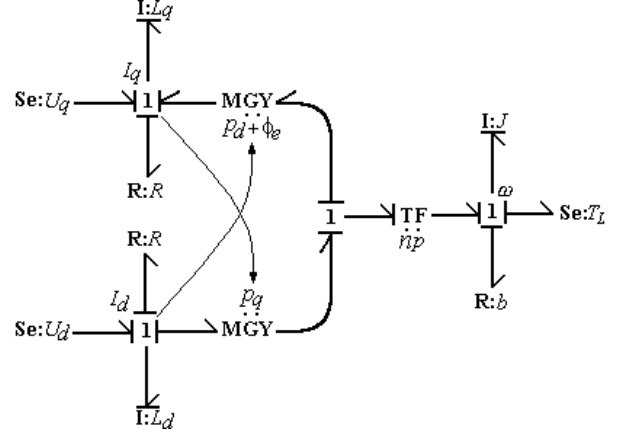


Figure 2. BG of the PMSM

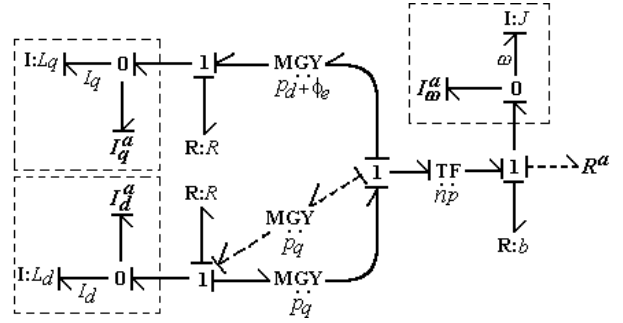


Figure 3. Target BG for the PMSM

The TBG dynamics is represented by (18). The  $S_{ij}^a$  matrices have been introduced in the model with the purpose of assigning the new interconnection structure and the desired dissipative function .

$$\dot{X}_i = \left\{ (S_{11} + S_{11}^a) + (S_{13} + S_{13}^a)l(X_i) \left[ I - (S_{33} + S_{33}^a)l(X_i) \right]^{-1} \right. \quad (18)$$

$$\left. (S_{31} + S_{31}^a) + S_{13}^{aa}l^a(X_i)S_{31}^{aa} \right\} (Z_i + Z_i^a)$$

The matrix  $S^a_{11}$  has the gains of the zero order causal paths from the outputs to the inputs of the storages that pass at least through one APB (Added Power Bonds, excluding that of the added storages). This matrix makes possible to assign new interconnections between the storages and contributes to the power conserving interconnection structure.

The following matrices allow to assign new dissipation to the system:  $S^a_{13}$  has the gains of the zero order causal paths from the outputs of the original resistors to the inputs of the storages.  $S^a_{33}$  has the gains of the zero order causal paths from the outputs to the inputs of the original resistors.  $S^a_{31}$  has the gains of the zero order causal paths from the outputs of the storages to the inputs of the original resistors.  $S^{aa}_{13}$  has the gains of the zero order causal paths from the outputs of the added resistors to the inputs of the storages.  $S^{aa}_{31}$  has the gains of the zero order causal paths from the outputs of the storages to the inputs of the added resistors.

All the causal paths considered have to pass at least through one APB in the TBG.

The function  $l^a(X_i)$  denotes the constitutive laws of the added resistors.

The desired closed loop dynamics (18) is obtained with a control law satisfying (19), the matching equation.

$$\begin{aligned} \left[ S_{14} + S_{13}l(X_i)(I - S_{33}l(X_i))^{-1}S_{34} \right] U = & [J_d(X_i) - R_d(X_i)]Z_i^a + \\ & + [J_a(X_i) - R_a(X_i)]Z_i \end{aligned} \quad (19)$$

with

$$\begin{aligned} J_d(X_i) - R_d(X_i) = & (S_{11} + S_{11}^a) + S_{13}^a l^a(X_i) S_{31}^{aa} + \\ & + (S_{13} + S_{13}^a)l(X_i) \left[ I - (S_{33} + S_{33}^a)l(X_i) \right]^{-1} (S_{31} + S_{31}^a) \end{aligned} \quad (20)$$

$$\begin{aligned} J_a(X_i) - R_a(X_i) = & S_{11}^a + S_{13}^a l^a(X_i) S_{31}^{aa} - S_{13}l(X_i) \left[ I - S_{33}l(X_i) \right]^{-1} S_{31} + \\ & + (S_{13} + S_{13}^a)l(X_i) \left[ I - (S_{33} + S_{33}^a)l(X_i) \right]^{-1} (S_{31} + S_{31}^a) \end{aligned} \quad (21)$$

Again as in ES, to stabilize a given state  $X_i^*$ , the shaped energy function has to be chosen such that it has a minimum at  $X_i^*$ .

*Remark 2.* The presence of coupled resistors can contribute to the power conservative interconnection structure (Donaire and Junco 2005) making unclear in the graph how to assign the desired interconnection or the dissipation function. In order to avoid this difficulty it can be useful to set  $S_{33}^a = -S_{33}$ . Then, the closed loop dynamics has not coupled resistors, its conservative interconnection structure is fully defined by the interconnection among the storages, and the dissipation is characterized by the resistors and their interconnection with the system. In this manner, it is clear that  $S_{11}^a$  is the added interconnection and  $S_{13}^a$ ,  $S_{31}^a$ ,  $S_{13}^{aa}$ ,  $S_{31}^{aa}$  and  $l^a(X_i)$  the added damping.

## EXAMPLES AND APPLICATIONS

Two practical cases are presented to illustrate the ES and IDA techniques in the BG domain. The first is the Boost Converter which has the particularity that the control acts through the structure (modulated control system). The output voltage regulation problem has been solved in (Ortega et al. 2002) using the ES theory on a PCHD-model. Here, the problem is revisited in the BG-domain with the only purpose of validation, showing that the method yields the same result. The second case is an application of the IDA method to the rotor speed regulation of the Excitation Controlled DC-Motor. New energy and dissipation functions are assigned to this port controlled system.

### Boost Converter

The BG of the averaged Boost Converter presented in Fig. 4 (Delgado et al. 1998) clearly shows that the control input, the duty cycle modulating the MTF, acts through the interconnection structure. The control objective is to regulate the capacitor voltage (the effort, in BG language) at a desired value  $V_C^* = q_C / C_1$  by a state feedback control law, maintaining internal stability.

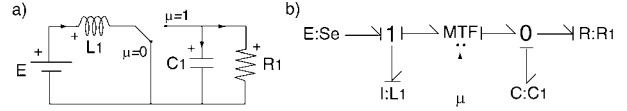


Figure 4. a) Boost Converter b) Averaged BG Model

The  $X_i$ ,  $Z_i$  and  $U$  vectors, and the matrices  $L$  and  $F$  are defined in (22), and the structure matrices of the JS in (23).

$$X_i = \begin{bmatrix} p_L \\ q_C \end{bmatrix}, Z_i = \begin{bmatrix} I_L \\ V_C \end{bmatrix}, U = E, L = \frac{1}{R_1} > 0, F = \begin{bmatrix} 1/L_1 & 0 \\ 0 & 1/C_1 \end{bmatrix} \quad (22)$$

$$S_{11} = \begin{bmatrix} 0 & -\mu \\ \mu & 0 \end{bmatrix}, S_{13} = \begin{bmatrix} 0 \\ -1 \end{bmatrix}, S_{31} = \begin{bmatrix} 0 & 1 \end{bmatrix}, S_{14} = \begin{bmatrix} 1 \\ 0 \end{bmatrix} \quad (23)$$

According with (13), the PCHD dynamics results in (24)

$$\dot{X}_i = \left\{ \begin{bmatrix} 0 & -\mu \\ \mu & 0 \end{bmatrix} - \begin{bmatrix} 0 & 0 \\ 0 & 1/R_1 \end{bmatrix} \right\} Z_i + \begin{bmatrix} 1 \\ 0 \end{bmatrix} E \quad (24)$$

In this example only the energy function will be changed to illustrate the BG-ES method. The TBG is built adding the storages (dashed-line box in Fig. 5) which contribute the energy necessary to obtain the desired energy function.

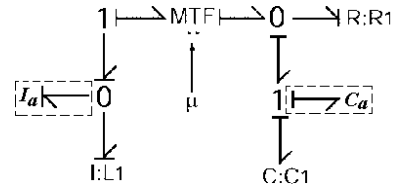


Figure 5. Target BG for the Boost Converter

The dynamics (25) of the TBG is the desired dynamics of the closed-loop system. It is a PCHD with the Hamiltonian (26). In this example, the relation (16) takes the form (27), which determines the control law.

$$\dot{X}_i = \left\{ \begin{bmatrix} 0 & -\mu \\ \mu & 0 \end{bmatrix} - \begin{bmatrix} 0 & 0 \\ 0 & 1/R_1 \end{bmatrix} \right\} (Z_i + Z_i^a) \quad (25)$$

$$H_d(X_i) = H(X_i) + H_a(X_i) \quad (26)$$

$$S_{14}U = [S_{11} + S_{13}LS_{31}]Z_i^a \Rightarrow \begin{cases} E = -\mu \frac{\partial H_a}{\partial q_C} \\ 0 = \mu \frac{\partial H_a}{\partial p_L} - \frac{1}{R_1} \frac{\partial H_a}{\partial q_C} \end{cases} \quad (27),$$

where  $Z_i^a = \partial H_a / \partial X_i$  is the gradient of the added energy function respect to the state variables. The control law (28) is obtained after solving the set of PDEs (27)

$$\mu = -E \left[ \frac{(2/R_1 E)C_1 p_L + C_2}{C_1 q_C + C_3} \right] \quad (28)$$

$C_{1,2,3}$  are constants to be determined such that  $H_a(X_i)$  satisfies (4), resulting in (29) and (30), or (29) and (31).

$$C_2 = -\left[2L_1(q^*/C_1)^2/R_1^2E^2\right]C_1 - \frac{C_3}{q^*/C_1} \quad (29)$$

$$C_3 < 0 \quad , \quad \frac{R_1^2EC_1^3}{4L_1q^{*3}} < C_1 < \frac{C_3}{q^*} \quad (30)$$

$$C_3 > 0 \quad , \quad -\frac{R_1^2EC_1^3}{4L_1q^{*3}} > C_1 > -\frac{C_3}{q^*} \quad (31)$$

The added energy (32) is the energy stored in  $I_a$  and  $C_a$ ; the constant  $C$  gives the possibility to force  $H_a(X_i^*)=H(X_i^*)+H_a(X_i^*)=0$ , thus qualifying  $H_a(X_i)$  as a Lyapunov function. The constitutive laws of the added elements are defined by (33) and (34) for the added inertia and capacitor, respectively. These equations show that  $I_a$  and  $C_a$  are nonlinear modulated storage elements.

$$H_a(p, q) = \frac{1}{2C_1} \frac{(C_1q + C_3)^2}{(2/R_1E)C_1p + C_2} + C \quad (32)$$

$$Z_p^a = f_p^a(X_i) = -R_1E(C_1q + C_3/2C_1p + R_1EC_2)^2 \quad (33)$$

$$Z_q^a = f_q^a(X_i) = R_1E(C_1q + C_3/2C_1p + R_1EC_2) \quad (34)$$

### Separately Excited DC – Motor

The DC-Motor is a port-controlled system as shows the BG in Fig. 6. The control input considered here is the excitation voltage that modulates the power exchange between the electrical and mechanical subsystems through the excitation circuit. The control objective is to drive de rotor speed to a constant value  $\omega^*$ , changing its natural damping and assuring internal stability. The load torque is considered constant and known.

The state vector  $X_i$ , the input vector  $U$ , as well as the constitutive laws of the resistors and the storages,  $L$  and  $F$  respectively, are given in (35). The matrices that define the JS are read from the BG and written in (36).

The BG-IDA method will be applied to achieve the control objective. At first, the TBG is created. The energy is shaped by the storages in the dashed-line boxes and the damping is increased by the added resistor (Figure 7). The added structure matrices read from the TBG and the constitutive law of the added resistor are in (37).

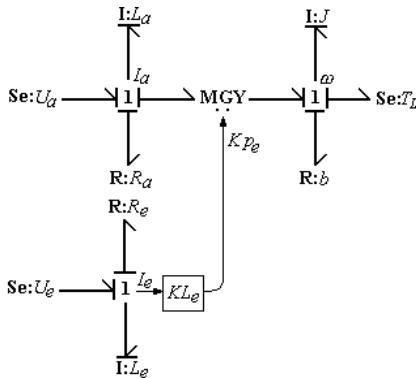


Figure 6. BG of the DC-Motor

$$X_i = \begin{bmatrix} p_a \\ p_e \\ p_\omega \end{bmatrix}, U = \begin{bmatrix} U_a \\ T_L \\ U_e \end{bmatrix}, L = \begin{bmatrix} R_a & 0 & 0 \\ 0 & b & 0 \\ 0 & 0 & R_e \end{bmatrix}, F = \begin{bmatrix} 1/L_a & 0 & 0 \\ 0 & 1/J & 0 \\ 0 & 0 & 1/L_e \end{bmatrix} \quad (35)$$

$$S_{11} = \begin{bmatrix} 0 & -Kp_e & 0 \\ Kp_e & 0 & 0 \\ 0 & 0 & 0 \end{bmatrix}, \quad S_{31} = \begin{bmatrix} 1 & 0 & 0 \\ 0 & 1 & 0 \\ 0 & 0 & 1 \end{bmatrix}$$

$$S_{14} = \begin{bmatrix} 1 & 0 & 0 \\ 0 & -1 & 0 \\ 0 & 0 & 1 \end{bmatrix}, \quad S_{13} = \begin{bmatrix} -1 & 0 & 0 \\ 0 & -1 & 0 \\ 0 & 0 & -1 \end{bmatrix} \quad (36)$$

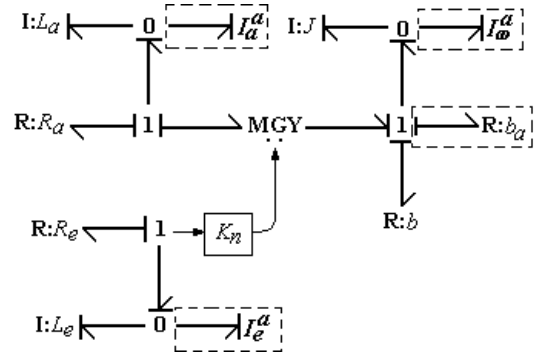


Figure 7. Target BG for the DC-Motor

$$S_{11}^a = S_{13}^a = S_{33}^a = S_{31}^a = 0_{3 \times 3}, S_{13}^{aa} = \begin{bmatrix} 0 \\ -1 \\ 0 \end{bmatrix}, S_{31}^{aa} = \begin{bmatrix} 0 & 1 & 0 \end{bmatrix}, L^a = b_a \quad (37)$$

The matching equation (19) results in the set of PDEs (38), that defines the control law.

$$\begin{cases} U_a = -K p_e \frac{\partial H_a}{\partial p_\omega} - R_a \frac{\partial H_a}{\partial p_a} \\ -T_L = -(b+b_a) \frac{\partial H_a}{\partial p_\omega} + K p_e \frac{\partial H_a}{\partial p_a} - b_a p_\omega \\ U_e = -R_e \frac{\partial H_a}{\partial p_e} \end{cases} \quad (38)$$

The first PDE of (38) is a first-order quasi linear partial differential equation. It can be solved with the method of characteristics (Elsoltz 1969) resulting that the added energy has the form (39)

$$H_a(X_i) = -\frac{U_a}{R_a} p_a + \varphi\left(\frac{K p_e p_a}{R_a} - p_\omega\right) + \gamma(p_e) + C \quad (39)$$

Where  $\varphi$  and  $\gamma$  are functions to be selected, and  $C$  is an arbitrary constant.

The second PDE of (38) gives the restriction (40) over the choice of  $\varphi$ .

$$\frac{\partial \varphi}{\partial \alpha} = \frac{K J U_a p_e - R_a J T_L + b_a R_a p_\omega}{J \left[ K^2 p_e^2 + (b+b_a) R_a \right]} \quad (40)$$

with  $\alpha = (K p_e p_a / R_a) - p_\omega$  being the argument of  $\varphi$ .

The third PDE of (38) defines the control law (41), the excitation voltage.

$$U_e = -R_e \frac{\partial \gamma}{\partial p_e} - R_e \frac{K p_a (b_a R_a p_\omega - J R_a T_L + J K U_a p_e)}{J R_a (K^2 p_e^2 + (b + b_a) R_a)} \quad (41)$$

The choice of  $\gamma$  is in agreement with the requirements of equilibrium and the minimum energy given in (9) and (10), respectively. For the DC-Motor given in Table 3, considering the desired equilibrium  $p_\omega^* = 981.747$  Kgm<sup>2</sup>/s (corresponding to the rated speed) and the added damping  $b_a = 2$  Nms;  $\gamma$  has to satisfy (42)

$$\left. \frac{\partial \gamma}{\partial p_e} \right|_{p_e^*} = -30.016 \quad \left. \frac{\partial^2 \gamma}{\partial p_e^2} \right|_{p_e^*} > 0.10225 \quad (42)$$

Accordingly, the law (43) is proposed

$$\gamma(p_e) = a_1 p_e^2 + a_2 p_e \quad (43)$$

with  $a_1 = 5$  and  $a_2 = -4097.2$ .

Thus, the control law is completely specified. The closed-loop is a PCHD system with the Hamiltonian  $H_d(X_i) = H(X_i) + H_a(X_i)$ ,  $H_d$  has a minimum at the desired state which is asymptotically stable. Consequently, the control objective has been satisfied.

The TBG representing the closed-loop system is shown in Figure 7. The constitutive laws of the added elements are given in (44)-(46), corresponding to  $I_a^a$ ,  $I_\omega^a$  and  $I_e^a$ , respectively.

$$f_1^a(X_i) = -\frac{U_a + K p_e}{R_a} - \frac{K J U_a p_e - R_a J T_L + b_a R_a p_\omega}{J [K^2 p_e^2 + (b + b_a) R_a]} \quad (44)$$

$$f_2^a(X_i) = -\frac{K J U_a p_e - R_a J T_L + b_a R_a p_\omega}{J [K^2 p_e^2 + (b + b_a) R_a]} \quad (45)$$

$$f_3^a(X_i) = 2a_1 p_e + a_2 + \frac{K p_a}{R_a} - \frac{K J U_a p_e - R_a J T_L + b_a R_a p_\omega}{J [K^2 p_e^2 + (b + b_a) R_a]} \quad (46)$$

## SIMULATION RESULTS

Simulation results are presented to verify the stability of the Excitation Controlled DC-Motor given in Table 3 (Pfaff 1990) with the control law (41).

Table 3. DC-Motor Data

Rated Power	147.2 Kw
Rated Speed	65.4498 s <sup>-1</sup>
Rated Armature Voltage $U_{an}$	460 v
Rated Armature Current $I_{an}$	320 A
Armature Resistance $R_a$	0.05 $\Omega$
Armature Inductance $L_a$	0.003 Hy
Excitation Resistance $R_e$	25.2 $\Omega$
Excitation Inductance $L_e$	63.5 Hy
Conversion Constant $K$	0.0166 Nm/WbA
Rotor Inertia $J$	15 Kgm <sup>2</sup>
Viscosity Coefficient $b$	3 Nms

It is well known that the DC-Motor variables could have dangerous overvalues if the machine is started up without necessary cautions. An usual strategy feeds the excitation first, and once the excitation flux established, supplies an armature ramp that saturates at rated voltage. In this simulation, once the armature voltage ramp reaches its rated value (Fig. 10.a), the load torque is connected to the motor (Fig. 9.b). The excitation voltage is injected from the very beginning according with the control law (41), but is limited to the rated value in order to protect the motor. Fig. 8.a shows that the evolution of the rotor speed has two parts. In the start-up period (0-5 sec.), the excitation voltage is at its limit value; thereafter (5-10 sec.), the action of the control law assures the regulation of the speed as well as the other states variables to the desired value (Figs. 8.b and 9.a).

These simulation results confirm the asymptotic stability of the Excitation Controlled DC-Motor in closed-loop under the control law (41), as it was predicted with the control theory of PCHD system in the BG domain.

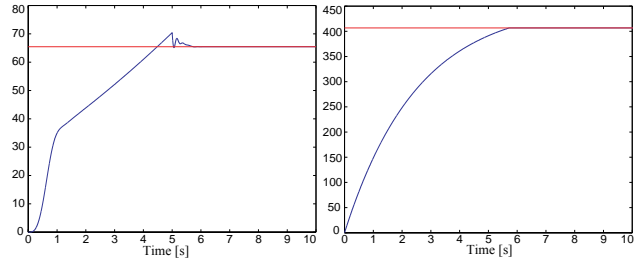


Figure 8. a) Rotor Speed b) Excitation Flux

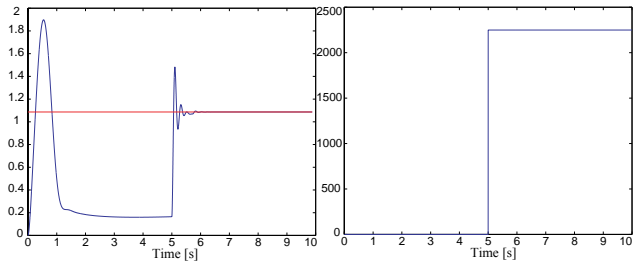


Figure 9. a) Armature Flux b) Load Torque

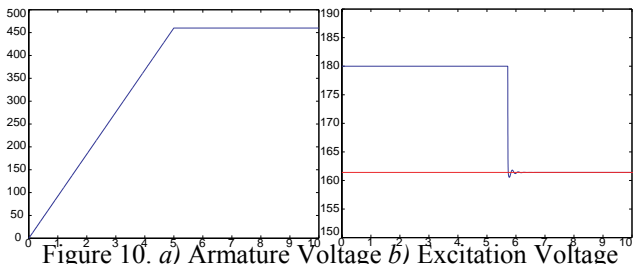


Figure 10. a) Armature Voltage b) Excitation Voltage

## CONCLUSIONS

The ES and IDA control techniques for PCHD have been interpreted in the BG domain for models with all the storages in ICA. The methodology is based on the representation of the desired closed-loop dynamics by a Target BG, which is built by adding components to the BG of the plant without control inputs. A set of PDE defining the control law is obtained by way of matching

the effect of the added components in the target BG with the action of the control inputs in the BG of the plant. The stabilization of a desired equilibrium is achieved solving the set of PDEs under the constraint of forcing a minimum of the closed-loop energy function at the desired equilibrium state.

Future research will focus on the transcription of ES and IDA techniques for BG models with storages in derivative causality assignment. It will be also looked for graphical strategies to add elements in the TBG with the purpose of solving the set of PDEs in a straightforward manner.

## REFERENCES

- Bertrand, J., Sueur, C. and Dauphin-Tanguy, G. 2001. "Input Output Decoupling with Stability for Bond Graph Models". *Nonlinear Dynamics and Systems Theory*, Vol. 1, N° 1, pp. 39-58.
- Dauphin-Tanguy, G., Rahmani, A. and Sueur, C. 1999. "Bond Graph Aided Design of Controlled Systems". *Simulation Practice and Theory* 7, N° 5-6 (December), pp. 493-513.
- Delgado, M. and Sira-Ramírez, H. 1998. "A bond graph approach to the modeling and simulation of switch regulates DC-to-DC power supplies". *Simulation Practice and Theory* 6, 7 (November), pp. 631-646.
- Donaire, A. and Junco, S. 2005. "Deriving Port-Controlled Hamiltonian Models with Dissipation From Bond Graphs". In *Proceedings of the 2005 International Conference on Integrated Modeling and Analysis in Applied Control and Automation* (Marseille, France, Oct. 20-22), pp. 117-126.
- Elsigoltz, L. 1969. *Ecuaciones Diferenciales y Cálculo Variacional*. MIR Editions, Moscow.
- Junco, S. 2004. "Virtual Prototyping of Bond Graphs Models for Controller Synthesis through Energy and Power Shaping." In *Proc. IMAACA'2004, the 2004 International Conference on Integrated Modeling and Analysis in Applied Control and Automation* (Bergeggi, Italy, October 28-31), Vol. 2, pp. 100-109.
- Karnopp, D., Margolis, D. and Rosenberg, R. 2000. *System Dynamics: Modeling and Simulation of Mechatronic Systems*, 3<sup>rd</sup> Edition. John Wiley and sons, New York.
- Ortega, R., van der Schaft, A., Maschke, B. and Escobar, G. 2002. "Interconnection and damping assignment passivity-based control of port-controlled Hamiltonian systems". *Automatica* 38, N° 4 (April), pp. 585-596.
- Pfaff, G. 1990. *Regelung Elektrischer Antriebe I, 4*. Oldenbourg Verlag Editions, München, Wien.
- Van der Schaft, A. 2000. *L<sub>2</sub>-Gain and Passivity Techniques in Nonlinear Control*, 2<sup>nd</sup> Edition. Springer-Verlag, London.
- Vink, D. 2005. *Aspects of Bond Graph Modelling in Control*. PhD Thesis, University of Glasgow, Scotland, UK (January).
- Willems, J. C. 1972. "Dissipative Dynamical Systems. Part I: General Theory". *Archive for Rational Mechanics and Analysis* 45, N° 5 (January), pp. 321-351.

## AUTHOR BIOGRAPHIES

**ALEJANDRO G. DONAIRE** was born in Rosario, Argentina. He received the undergraduate degree in Electronic Engineering from the Universidad Nacional de Rosario (UNR), Argentina, in 2003. Since April

2003 he has been a PhD student in Electronic Engineering and Control at the Faculty of Engineering (FCEIA) of UNR under the supervision of Prof. S. Junco. His work is supported by The Argentine National Council of Scientific and Technical Research (CONICET). He had two short research stages at LAGIS, Ecole Centrale de Lille, France, in 2003 and 2004. He was a teaching assistant in two undergraduate courses, one on System Dynamics and Control and the other on Control of Electrical Drives, both at FCEIA-UNR. His main research interests are on Bond Graphs, Nonlinear Control, and Motion Control Systems. E-mail address: adonaire@fceia.unr.edu.ar. His laboratory's web-page is: <http://www.fceia.unr.edu.ar/lsd/people>.

**SERGIO J. JUNCO** was born in Rafaela, Argentina in 1951. He received the Electrical Engineer degree from UNR in 1976. From 1976 to 1979, he worked on automation projects as an Electronic Project Engineer at Acindar, a large private steel company in Argentina. From 1979 to 1981, he was at the Institute of Automatic Control of the University of Hannover, Germany, with a scholarship from DAAD (the German Academic-Exchange Service). In September 1982, he joined the National University of Rosario, where he currently is an Associate Professor of System Dynamics and Control and Head of the Department of Electronics. He has held several invited positions at research labs and universities in Spain and France. Prof. Junco is a member of AADECA, IEEE, IFAC and SCS. His current research interests are in modeling, simulation, control and diagnose of dynamic systems, with applications in the fields of motion control systems with electrical drives, power electronics, mechatronics and vehicle dynamics. He has developed, and currently teaches, several courses at both undergraduate and graduate level on System Dynamics, Bond Graph Modeling and Simulation, Advanced Nonlinear Dynamics and Control of Electrical Drives, as well as Linear and Nonlinear Control with Geometric Tools.